Chemical Engineering Science 188 (2018) 192–207

Contents lists available at ScienceDirect

Chemical Engineering Science

journal homepage: www.elsevier.com/locate/ces

Thermal stability criterion integrated in model predictive control for batch reactors

Walter Kähm, Vassilios S. Vassiliadis *

Department of Chemical Engineering and Biotechnology, Process Systems Engineering Group, University of Cambridge, West Cambridge Site, Philippa Fawcett Drive, CB3 0AS Cambridge, UK

HIGHLIGHTS

- Limitations of current stability criteria for thermal runaway detection identified.
- Novel stability criterion for more reliable runaway detection is proposed and tested.
- Online integration of stability criterion into MPC scheme.
- New robust scheme for optimising control with improved stability performance.
- Illustrative case studies with large improvements to stability and productivity.

GRAPHICAL ABSTRACT

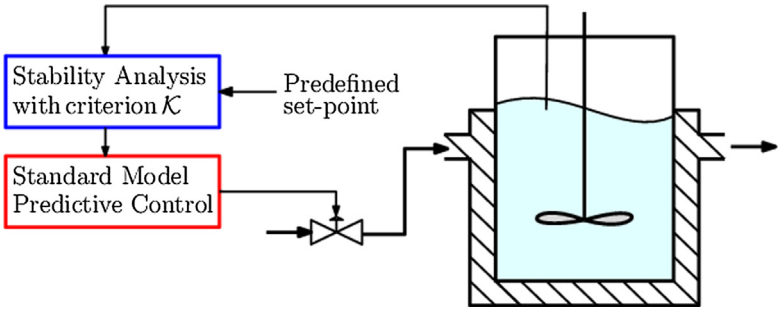

ARTICLE INFO

Article history:
Received 27 July 2017
Received in revised form 18 April 2018
Accepted 18 May 2018
Available online 19 May 2018

Keywords:
Thermal stability criterion
Thermal runaway detection
Model predictive control
Intensification of batch processes

ABSTRACT

Thermal runaways can have a significant impact on the performance and normal operation of reaction processes, causing safety issues and financial loss, which hinder the intensification of such processes. More specifically, a control system that does not possess proper detection mechanisms of the boundary of stability will by necessity be overly conservative. This leads to poorer performance and the inability to intensify the process, *i.e.* to reduce process times for example and also to achieve higher yields.

For the intensification of batch processes a stability criterion, based on the divergence criterion, is presented. The derivation of the stability criterion and a comparison to the original divergence criterion is shown for several batch reactions. It is shown that the stability criterion classifies the system behaviour more reliably for the case studies considered. This stability criterion is embedded in Model Predictive Control, which is a novel control scheme. This scheme allows the controlled increase of the reaction temperature while keeping the processes in a stable region, hence reducing the risk of thermal runaways. This control system enables batch processes to achieve a target conversion in a reduced completion time of reaction and an intensification of batch processes.

1. Introduction

The reaction temperature for exothermic batch processes is evaluated from the point of view of the thermal and chemical stability, as well as reaction safety. The chemical stability temperature T_{chem} sets boundaries for the chemical consumption of reactants and production of large amounts of unwanted side products in reactors. The thermal stability of batch processes will be evaluated with given reaction kinetics, energy and mass balances, as well as cooling intensity and reactor parameters. In most exothermic

* Corresponding author.
E-mail address: vsv20@cam.ac.uk (V.S. Vassiliadis).

https://doi.org/10.1016/j.ces.2018.05.032
0009-2509/

Nomenclature

$\mathbf{J}$	Jacobian matrix [–]
$\mathbf{M}$	matrix of coefficients for linear differential equation [–]
ΔH_r	enthalpy of reaction [kJ mol^{-1}]
ϵ_{tol}	ODE solver tolerance [–]
γ	Arrhenius number [–]
Λ	Lyapunov exponent [s^{-1}]
λ	thermal conductivity [W m^{-1} K^{-1}]
[A], [B], [C]	concentration of components A, B, and C [kmol m^{-3}]
$\mathcal{E}$	divergence estimate at boundary of stability [s^{-1}]
$\mathcal{K}$	stability criterion [s^{-1}]
μ	viscosity [Pa s]
Φ	objective function for Model Predictive Control [K^2 s]
ρ, ρ_C	density of reactor contents and coolant, respectively [kg m^{-3}]
τ_I	integral constant for PI control [K s^2 m^{-3}]
ε	small perturbation [–]
A	heat transfer area [m^2]
B	dimensionless adiabatic temperature rise [–]
C_p, C_{pC}	heat capacity of reaction mixture and coolant, respectively [kJ kg^{-1} K^{-1}]
Da	Damköhler number [–]
E_a	activation energy [J mol^{-1}]
h	equations for physical properties of reaction mixture [–]
i	current time step [–]
J_{jl}	Jacobian matrix entry (row j, column l) [–]
k_0	reaction rate constant [(m^3 kmol^{-1})$^{n-1}$ s^{-1}]
K_p	proportional constant for PI control [m^3 s^{-1} K^{-1}]
$m_B, m_{Da}, m_\gamma, m_{St}$	coefficients for stability function $\mathcal{K}$ [–]
N	number of differential equations [–]
n	reaction order with respect to component A [–]
q_C	coolant flow rate [m^3 s^{-1}]
Q_{gen}	heat generated by reaction [W]
R	universal molar gas constant [J mol^{-1} K^{-1}]
r	reaction rate [kmol m^{-3} s^{-1}]
St	Stanton number [–]
t	time [s]
t'	dummy variable for integration [s]
T_{chem}	temperature of chemical stability boundary [K]
T_R, T_C, T_{sp}	temperature of reactor contents, coolant and reaction set point, respectively [K]
U	heat transfer coefficient [W m^{-2} K^{-1}]
V, V_C	volume of reactor and cooling jacket, respectively [m^3]
x	differential variable [–]
X_A	conversion of component A [–]
$y_j, \bar{y}_j, \hat{y}_j$	mass fraction, mole fraction and volume fraction of component j, respectively [–]

batch reactions the thermal stability is the limiting factor (Westerterp and Molga, 2006).

In batch reactions the reactor temperature T_R is usually controlled by Proportional-Integral-Derivative (PID) or Proportional-Integral (PI) control during the whole process (Stephanopoulos, 1984; Winde, 2009). Depending on the heat generation the PID/PI controller regulates the coolant flow to keep a constant reaction temperature. As the reaction proceeds, more reactants are consumed and therefore the heat generation decreases.

The chemical reaction can be intensified by increasing the temperature during the reaction. This leads to a faster completion time for the reaction, at which the required conversion, e.g. $X_{A,end} = 0.95$, is achieved. A higher temperature throughout a reaction process leads to a faster reaction, making the time required to reach the target conversion smaller. This in turn means that, for the notation used in Fig. 1, $t_1 < t_2$, since the temperature for process 1 is increased continuously. The chemical stability boundary of $T_{chem} = 425$ K must not be surpassed in order to reduce side product formation. The process intensification for batch reactions is schematically shown in Fig. 1. The lines shown in Fig. 1 are for illustration purposes and have no relation to the processes considered in the following sections.

Model Predictive Control (MPC) is a more advanced control system, capable of considering system bounds (Rawlings and Mayne, 2015). This type of control system is successfully used in industry for many applications (Mayne, 2014). The thermal stability of a process can therefore be connected to MPC to achieve higher stability for the reaction.

The inclusion of a stability criterion was carried out in Rossi et al. (2015) in a slightly different way: an algorithm was found which determines when the system is in a stable regime, giving rise to a Boolean variable which switches according to the state of the system. This Boolean variable hence 'activates' an additional term within the objective function, therefore penalising the control if the system drifts into an unstable regime. The function defining

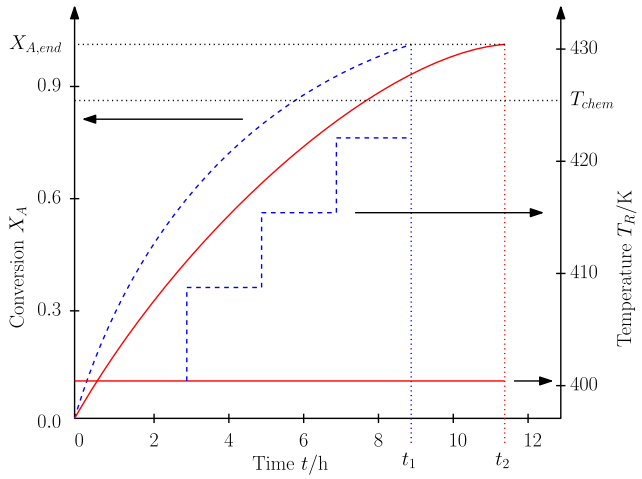

Fig. 1. Schematic of temperature and conversion profiles for batch reactions with (blue lines) and without (red lines) set point changes in temperature. (For interpretation of the references to color in this figure legend, the reader is referred to the web version of this article.)

this Boolean variable depends on the system under consideration. This approach can potentially lead to badly scaled problems. A similar approach was tested in this work for the stability criterion $\mathcal{K}$: it was found that tuning the scaling requires a lot of trial and error. In this work this problem does not exist, since the stability criterion is added as a nonlinear constraint.

This work introduces a suitably modified stability criterion in a totally novel way, such that it can be integrated in Model Predictive Control algorithms in a seamless manner. Case studies demonstrate the validity of the approach and the enhanced performance gained over more traditional PID control systems and MPC algorithms without such embedded stability criteria.

The following analyses are required to achieve the new scheme:

- simulation of exothermic batch reactors as a basis for MPC
- investigation of suitable methods to evaluate stability for the application to MPC
- definition of a function for the thermal stability in batch reactors
- implementation of this function in MPC

2. Simulation of batch processes

In the model used for the subsequent simulations of batch processes, exothermic and irreversible reactions of order $n = 1$ to $n = 3$ are analysed

$$\mathrm{A} + \mathrm{B} \rightarrow \mathrm{C} \tag{2.1}$$

The model of the batch processes is based on differential equations for mass and energy balances. The reaction kinetics mainly consider component A with a reaction order n, which are assumed to follow the Arrhenius equation (Davis and Davis, 2003). Examples of reactions with this kinetic scheme are polycondensation reactions, e.g. of dicarboxylic acid and diols, or the addition reaction for the synthesis of ethylene glycol from ethylene oxide and water. A diagram of the batch reactor system including PI control is shown in Fig. 2.

The mass balance for each component is given by:

$$\frac{\mathrm{d}[\mathrm{A}]}{\mathrm{d}t} = -r([\mathrm{A}], T_R) \tag{2.2}$$

$$\frac{\mathrm{d}[\mathrm{B}]}{\mathrm{d}t} = -r([\mathrm{A}], T_R) \tag{2.3}$$

$$\frac{\mathrm{d}[\mathrm{C}]}{\mathrm{d}t} = +r([\mathrm{A}], T_R) \tag{2.4}$$

$$r([\mathrm{A}], T_R) = k_0 [\mathrm{A}]^n \exp\left(-\frac{E_a}{R T_R}\right) \tag{2.5}$$

where n is the order of reaction with respect to component A. The energy balance for the reactor contents are given by:

$$\frac{\mathrm{d}}{\mathrm{d}t}(V \rho C_p T_R) = r([\mathrm{A}], T_R)(-\Delta H_r) V - UA(T_R - T_C) \tag{2.6}$$

The energy balance for the cooling jacket is given by:

$$\frac{\mathrm{d}}{\mathrm{d}t}(V_C \rho_C C_{pC} T_C) = q_C \rho_C C_{pC}(T_{C,in} - T_C) + UA(T_R - T_C) \tag{2.7}$$

The heat generation due to the stirrer is assumed to be 10 W m^{-3}, which is ignored due to the small value compared to the other terms in the energy balances. This is the case due to the low viscosity of the reaction mixture, which mainly contains water. For reaction mixtures with a higher viscosity, the heat generated by the stirrer cannot be neglected.

The physical properties of components A, B and C used in the simulations are shown in Table 1.

The changes in density, viscosity and heat capacity of the reaction mixture with changing temperature and composition are approximated in the simulation. Depending on the composition the following equations are used to estimate the physical properties of the reaction mixture:

$$\frac{1}{\rho} = \sum_j y_j / \rho_j \tag{2.8}$$

$$\ln \mu = \sum_j \bar{y}_j \ln \mu_j \tag{2.9}$$

$$C_p = \sum_j y_j C_{pj} \tag{2.10}$$

$$\lambda = \sum_j \hat{y}_j \lambda_j \tag{2.11}$$

where y_j is the mass fraction, $\bar{y}_j$ is the molar fraction, and $\hat{y}_j$ is the volume fraction of component j. These equations are obtained from Hirschfelder et al. (1955),Teja (1983) and Green and Perry (2008).

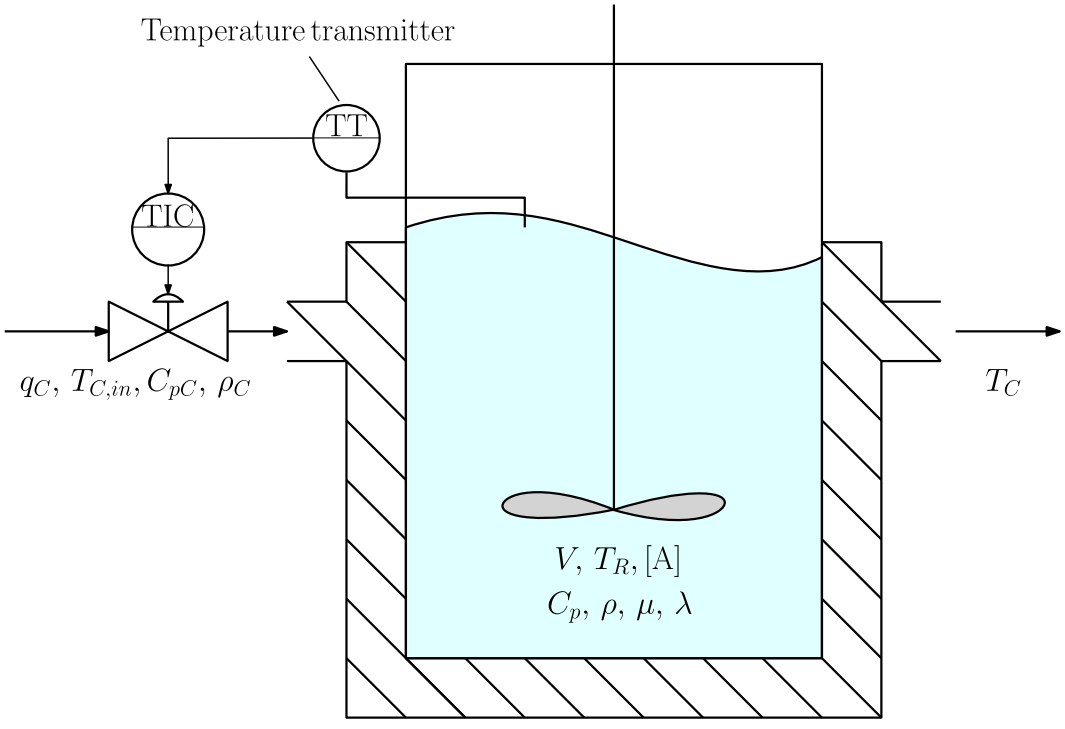

Fig. 2. Diagram of batch reactor with cooling jacket used for simulations.

Table 1
Physical constants for each component considered in batch processes.

Component	ρ [kg m^{-3}]	μ [Pa s]	C_p [kJ kg^{-1} K^{-1}]	λ [W m^{-1} K^{-1}]
A	590	1.0×10^{-4}	1.10	0.30
B	937	2.3×10^{-4}	4.20	0.69
C	1013	5.0×10^{-4}	2.40	0.35

Table 2
Process parameters for batch reactor simulations.

Parameter	V [m^3]	V_c [m^3]	A [m^3]	$T_{C,in}$ [K]	E_a/R [K]	$q_{c,max}$ [m^3 s^{-1}]
Value	16	1.2	30.7	300	9525	0.037

Table 3
Parameters for PI controller used in case studies.

Parameter	Value
Proportional (P), K_p	10 m^3 s^{-1} K^{-1}
Integral (I), τ_I	1000 K s^2 m^{-3}

Table 4
Reaction data for processes P_1—P_5.

Process	k_0 [(m^3 kmol^{-1})$^{n-1}$ s^{-1}]	n	ΔH_r [kJ mol^{-1}]	$[A]_0$ [kmol m^{-3}]
P_1	2.76×10^6	1.0	−75.0	13.0
P_2	7.65×10^5	1.5	−75.0	13.0
P_3	2.12×10^5	2.0	−75.0	13.0
P_4	5.89×10^4	2.5	−75.0	13.0
P_5	3.06×10^4	3.0	−75.0	13.0

The accurate description of the temperature and composition relationships for liquid mixtures is very difficult. Hence, for the change in temperature linear interpolation of tabulated physical properties for water, ethylene oxide and ethylene glycol, components A, B and C respectively, are used. The temperature dependence of the above parameters is obtained from Dever et al. (2004), Crittenden et al. (2012) and Bohne et al. (2010).

The heat transfer coefficient U of the reaction mixture to the cooling jacket is evaluated from the properties of the reaction mixture and the coolant, as well as the flow rate of coolant (Sinnot, 2005). The remaining process parameters are given in Table 2.

In the first set of case studies the reaction order with respect to reagent A and the enthalpy of reaction are varied. The batch reactor temperature is controlled by varying the cooling water flow rate q_C with a PI controller. The equation of the PI controller used is given by the following equation:

$$q_C(t) = K_p\left(T_R(t) - T_{sp}(t)\right) + \frac{1}{\tau_I}\int_{t_0}^{t}\left(T_R(t') - T_{sp}(t')\right)dt' \tag{2.12}$$

where K_p is the proportional parameter, τ_I is the integral parameter, $T_{sp}(t)$ is the set point temperature at time t and t' is a dummy variable.

The tuning parameters of the PI controller used are not of major importance for the processes considered. The main point of the PI controller is to give relatively quick response to temperature set point changes. Hence it is not necessary to have a perfectly tuned PI controller. It is of greater importance in this work to see where the system becomes unstable. To achieve such a behaviour the tuning coefficients were obtained by trial and error. The parameters of the PI controller used are given in Table 3.

All simulations shown in this paper were carried out on an HP EliteDesk 800 G2 Desktop Mini PC with an Intel® Core™ i5-65,000 processor, with operating system Windows 7 Enterprise. The system dynamics were simulated using *ode15s* (Shampine et al., 1999) within MATLAB™. MATLAB™ was used due to its simplicity of developing code. If the computational time for each iteration needs further improvement, more efficient programming languages as C, C++ and FORTRAN can potentially be used.

The first set of case studies considers processes P_1—P_5. The reaction data for these processes are given in Table 4.

The temperature profiles for processes P_1—P_5 are shown in Fig. 3. After some time the first increase in temperature occurs. This increase in temperature is caused by a reduction of cooling water controlled by a PI controller. After this increase in intensification of the reaction, more coolant is required by the PI controller in order to keep the reaction temperature constant. At this point processes P_1—P_5 are still stable.

A further increase in set point temperature leads to an uncontrollable increase in reactor temperature. The cooling capacity is not enough to remove the heat generated by each reaction. Therefore processes P_1—P_5 are now unstable.

The process parameters for the boundary of instability were also determined for processes P_6—P_{15}. The reaction data for these processes are shown in Table 5.

For processes P_6—P_{15} the temperature is also controlled by the PI controller with parameters given in Table 3. The temperature for these processes follows a similar profile with an initially stable region which becomes unstable with an increase in set point temperature.

The evaluated process parameters for the transition to instability in the above processes are the foundation for the classification and determination of the thermal stability of batch reactions.

3. Analysis of stability criteria

The subject of thermal stability was first introduced in the theory of heat explosions (Semenov, 1940), which set the theoretical foundation. The introduction of more factors as the extent of heat generation and cooling intensity were introduced by Barkelew (1959), which enabled the evaluation of thermal stability for engineering purposes. These analyses were restricted to steady states, which makes them unfeasible for an implementation with advanced control systems.

Lyapunov exponents were used by Strozzi and Zaldívar (1994) for the determination of process stability in nonlinear dynamic systems. In this analysis every system variable considered has a Lyapunov exponent Λ associated with it. The value of Λ shows how sensitive the respective variable is to an initial perturbation ε. For the reaction temperature T_R the exponent is calculated by the following equation (Melcher, 2003):

$$\exp\left(\Lambda\left(T_R|_{t_0}\right) \times t\right) = \frac{|T_R\left(t, T_R|_{t_0}\right) - T_R\left(t, \varepsilon + T_R|_{t_0}\right)}{\varepsilon} \tag{3.1}$$

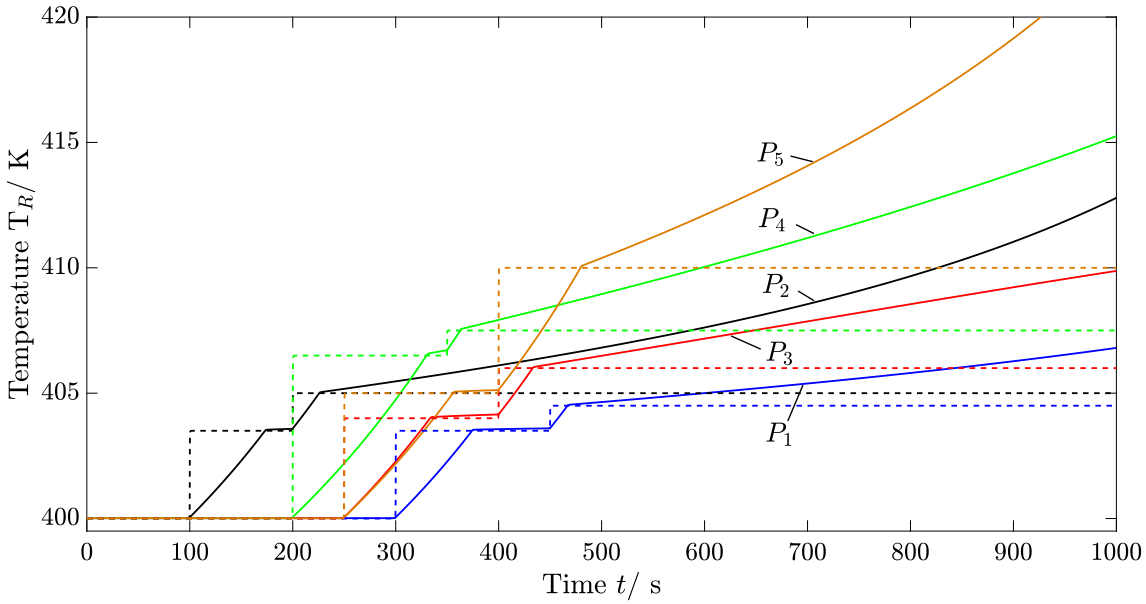

Fig. 3. Temperature profiles of processes P_1–P_5, the parameters of which are given in Table 4.

Table 5
Reaction data for processes P_6–P_{15}.

Process	k_0 $[(m^3\ kmol^{-1})^{n-1}\ s^{-1}]$	n	$\Delta_r H$ [kJ mol^{-1}]	$[A]_0$ [kmol m^{-3}]
P_6	2.76×10^6	1.0	−130.0	8.0
P_7	9.76×10^5	1.5	−110.0	8.0
P_8	3.45×10^5	2.0	−90.0	8.0
P_9	1.22×10^5	2.5	−75.0	8.0
P_{10}	4.31×10^4	3.0	−70.0	8.0
P_{11}	2.76×10^6	1.0	−75.0	8.0
P_{12}	2.76×10^6	1.0	−75.0	9.0
P_{13}	2.76×10^6	1.0	−75.0	11.0
P_{14}	2.76×10^6	1.0	−75.0	13.0
P_{15}	2.76×10^6	1.0	−75.0	15.0

The variation of the Lyapunov exponent $\Lambda\left(T_R|_{t_0}\right)$ with time gives information about the stability of the process at point t_0. If the exponent value is negative, the perturbed and unperturbed profiles converge. If the value for $\Lambda\left(T_R|_{t_0}\right)$ becomes positive, an unstable process is present at time t_0.

After taking logarithms on both sides, the following expression is obtained:

$$\Lambda\left(T_R|_{t_0}\right) = \frac{1}{t}\ln\frac{|T_R\left(t, T_R|_{t_0}\right) - T_R\left(t, \varepsilon + T_R|_{t_0}\right)}{\varepsilon} = \lim_{t\to\infty}\frac{1}{t}\ln\left|\frac{\delta T_R\left(t, T_R|_{t_0}\right)}{\delta T_{R,0}}\right| \tag{3.2}$$

The Lyapunov exponent $\Lambda\left(T_R|_{t_0}\right)$ therefore gives information about the stability at point t_0 only, which depends on how large the value of t becomes. In practice it is not possible to simulate the system until $t \to \infty$, and hence a local Lyapunov is evaluated instead, for which $t \to t_f$ where t_f is the final time, set to be very large. It is noted, that as $t \to \infty$, the Lyapunov exponent value tends towards the eigenvalues of the Jacobian.

In order to not miss a thermal runaway, the Lyapunov exponent at time t_0 has to be checked for many values of t_f. Otherwise the thermal runaway can potentially be overlooked and a stable reaction is assumed. Therefore a lot of simulations are required to scan for instability, which leads to a high computational cost. For this reason the Lyapunov exponent method is ruled out as an efficient stability criterion for the integration with MPC.

The divergence criterion, which is based on Liouville's theorem (Arnold, 1973), can be used for the analysis of stability for linear systems. Consider the following linear differential equation:

$$\dot{x} = \mathbf{M}x \tag{3.3}$$

For this system the divergence criterion is given by:

$$\mathrm{div}[\mathbf{M}] = \mathrm{tr}[\mathbf{M}] < 0 \tag{3.4}$$

Here tr[**M**] is the trace of matrix **M**, which is the sum of all diagonal elements in **M**. The system present in Eqs. (2.2)–(2.7) is stable when the divergence is negative (Strozzi and Zaldívar, 1999). According to Strozzi and Zaldívar (1999) the change from a stable to an unstable system occurs at a sign change of the divergence. This criterion does not require as many evaluations as the Lyapunov exponent and therefore promises to be a more practical measure of stability, which can be connected with MPC.

For nonlinear systems, a linear approximation can be made by using a Taylor expansion. Consider a set of differential equations:

$$\dot{x}_1 = f_1(x, t) \tag{3.5}$$

$$\dot{x}_2 = f_2(x, t) \tag{3.6}$$

$$\vdots \quad \vdots \quad \vdots$$

$$\dot{x}_N = f_N(x, t)$$

where N is the number of differential variables $\dot{x}$.

This leads to the following linear approximation:

$$\dot{x} = \mathbf{J}x \tag{3.8}$$

where **J** is the Jacobian matrix including all first order derivatives. The entry at row j and column l, J_{jl}, is evaluated by the following expression:

$$J_{jl} = \frac{\partial f_j}{\partial x_l} \tag{3.9}$$

The trace elements of the Jacobian matrix, which are the diagonal entries of **J**, for the system given in Eqs. (2.2)–(2.7) are therefore given by:

$$J_{11} = \frac{\partial\left[\dot{\mathrm{A}}\right]}{\partial[\mathrm{A}]} = -n\,k_0 \exp\left(\frac{-E_a}{RT_R}\right)[\mathrm{A}]^{n-1} \tag{3.10}$$

$$J_{22} = \frac{\partial\left[\dot{\mathrm{B}}\right]}{\partial[\mathrm{B}]} = 0 \tag{3.11}$$

$$J_{33} = \frac{\partial\left[\dot{\mathrm{C}}\right]}{\partial[\mathrm{C}]} = 0 \tag{3.12}$$

$$J_{44} = \frac{\partial \dot{T}_R}{\partial T_R} = \frac{1}{\rho C_p V}\left(\frac{k_0 E_a V(-\Delta H_r)}{RT_R^2}\exp\left(\frac{-E_a}{RT_R}\right)[\mathrm{A}]^n - UA\right) \tag{3.13}$$

$$J_{55} = \frac{\partial \dot{T}_C}{\partial T_C} = \frac{-1}{\rho_C C_{pC} V_C}\left(\rho_C C_{pC} q_C + UA\right) \tag{3.14}$$

According to Copelli et al. (2014) and Bosch et al. (2004), the main contributing factors for a thermal runaway are only those variables which occur in the heat generation Q_{gen} in the reactor energy balance. In this case study this is represented by the following expressions:

$$Q_{gen} = k_0 \exp\left(\frac{-E_a}{RT_R}\right)[\mathrm{A}]^n\,(-\Delta H_r)\,V \tag{3.15}$$

Therefore, the state variables of interest are [A] and T_R, as these are the contributors for the heat generated by the exothermic reaction. The cooling jacket temperature T_C will always give a negative contribution for the divergence, as can be seen in the expression for J_{55} in Eq. (3.14). The coolant temperature, as well as the concentrations of components B and C also do not appear in Eq. (3.15). Therefore the terms J_{22}, J_{33} and J_{55} are to be omitted for the divergence calculation, as given in Bosch et al. (2004) and Copelli et al. (2014). For this reason the following equation will be used to evaluate the divergence:

$$\begin{aligned}\mathrm{div}[\mathbf{J}] = J_{11} + J_{44} \Rightarrow \mathrm{div}[\mathbf{J}] &= -n\,k_0 \exp\left(\frac{-E_a}{RT_R}\right)[\mathrm{A}]^{n-1} \\ &+ \frac{1}{\rho C_p V}\left(\frac{k_0 E_a V(-\Delta H_r)}{RT_R^2}\exp\left(\frac{-E_a}{RT_R}\right)[\mathrm{A}]^n - UA\right)\end{aligned} \tag{3.16}$$

The divergence profiles for processes P_1—P_5 are shown in Fig. 4.

The divergence initially decreases with time due to the reduction in concentration of component A with time, and therefore a reduction in heat generated. The divergence increases after the first step change in the set point temperature occurs due to an increase in temperature. After the step change the divergence starts decreasing again as the concentration of reagent A decreases. Processes P_1—P_5 are still stable after their respective first increase in set point temperature.

A second increase in temperature set point leads to thermal runaways for each of the processes mentioned. As can be seen in Fig. 4 the divergence profiles all increase due to the uncontrolled increase in reactor temperature. After the second increase in set point temperature processes P_1—P_5 are unstable, since the temperature is running away.

The function div[J] for processes P_6—P_{15} follows a similar profile as processes P_1—P_5. The values of the divergence of the Jacobian matrix at the boundary of instability for processes P_1—P_{15} are given in Table 6.

Each individual component of the diagonal in the Jacobian matrix contributes towards the divergence. Every derivative in the Jacobian matrix is effectively a sensitivity with respect to each variable. Batch processes are not at steady state, therefore sensitivities are not zero. The sensitivity with respect to temperature turns out to be the largest in value, as well as positive, making the overall divergence positive. This is the case for most batch reaction processes, making the divergence criterion unsuitable as a stability criterion.

The values of the divergence criterion, as shown in Fig. 4, are of the order of 10^{-3}. This is not due to numerical effects of the ODE solver employed, since the divergence is evaluated with algebraic expressions (Eq. (3.16).

To prove this point, a sensitivity analysis of process P_5 is carried out with varying tolerances for the ODE solver employed. The tolerances ϵ_{tol} used, from lowest to highest accuracy, are $\epsilon_{tol} = 10^{-4}, 10^{-6}, 10^{-8}, 5\times10^{-9}, 2.5\times10^{-9}$. The simulation using the highest accuracy, namely $\epsilon_{tol} = 2.5\times10^{-9}$, is used as the reference. The error with respect to the reference trajectory is plotted on a logarithmic scale in Fig. 5.

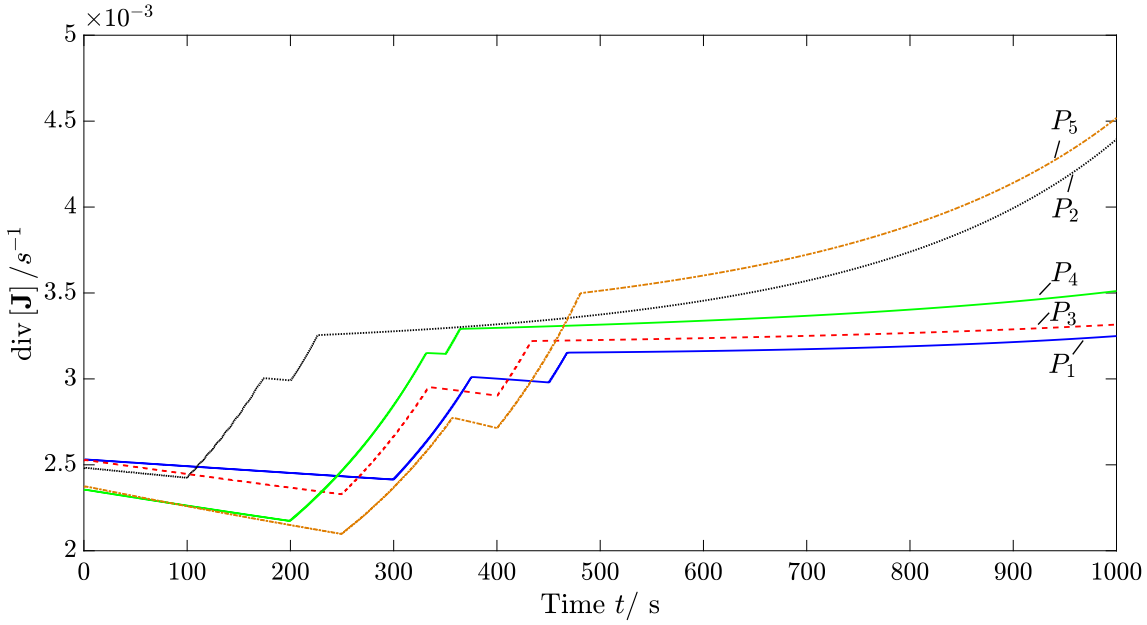

Fig. 4. Divergence profiles for processes P_1—P_5.

Table 6
Summary of divergence values at the boundary of instability for processes P_1—P_{15}.

Process	div[**J**]/10^{-3} [s^{-1}]	Process	div[**J**]/10^{-3} [s^{-1}]	Process	div[**J**]/10^{-3} [s^{-1}]
P_1	3.15	P_6	3.20	P_{11}	2.78
P_2	3.25	P_7	3.53	P_{12}	2.61
P_3	3.22	P_8	3.65	P_{13}	2.59
P_4	3.30	P_9	3.79	P_{14}	2.56
P_5	3.50	P_{10}	3.80	P_{15}	2.52

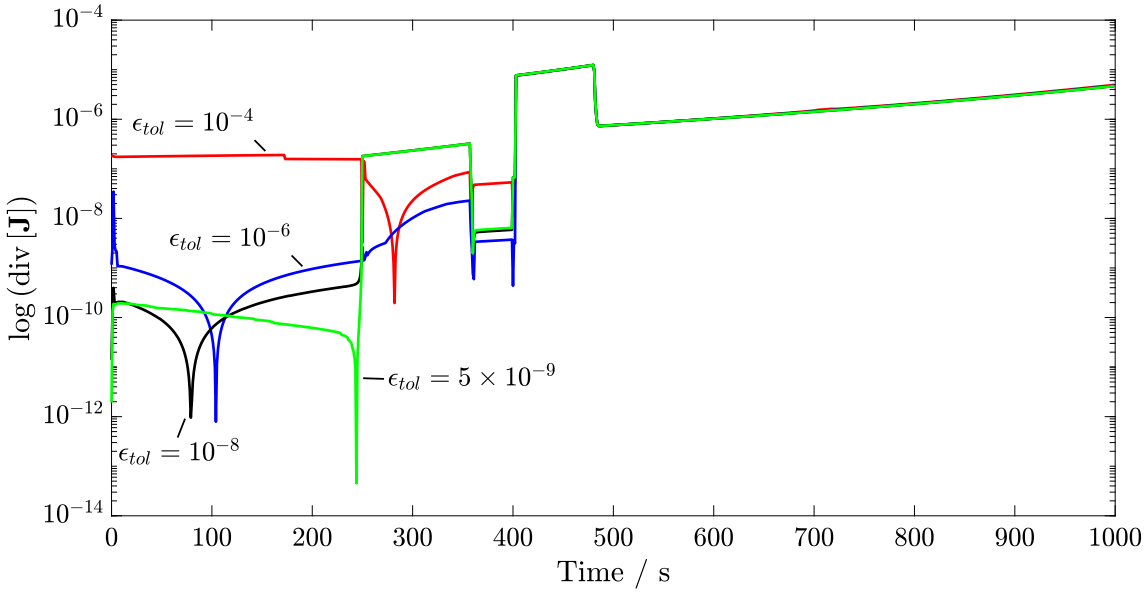

Fig. 5. Logarithmic plot of error profiles for each sensitivity setting.

As can be seen in Fig. 5 the errors are initially of the scale of 10^{-7}. As the process becomes unstable, each tolerance used results in an error of 10^{-5} which is approximately 1% of typical divergence values obtained. Hence the ODE tolerance settings do not cause the divergence to be positive for stable processes, but the nature of batch processes, where there is no steady state, causes the divergence to be in the positive region.

The tolerance setting used throughout all simulations is $\epsilon_{tol} = 10^{-8}$. As can be seen from Fig. 5 the error for the divergence obtained before loss of stability is approximately 10^{-8}—10^{-9}. Hence, the numerical effects due to the ODE solver used do not cause the divergence to be positive during stable operation.

The above simulations show the following results:

- the divergence can have positive values for stable batch processes
- the loss of stability does not occur at div[**J**] = 0
- the value of the divergence increases more drastically for unstable processes.

The values of the divergence do not enable to make quantitative conclusions about the stability of the system. Hence a new criterion is required for this purpose.

4. Function for stability criterion in batch reactors

4.1. Theory

The stability criterion $\mathcal{K}$ is introduced to define the boundaries of instability for exothermic batch reactions. This new function corrects the divergence of the Jacobian to obtain a clear statement about the system's stability. The stable region of a process is defined by:

$$\mathcal{K} \leqslant 0 \tag{4.1}$$

The significance of $\mathcal{K} = 0$ is that the system is on a limit cycle and therefore on the boundary of instability. The unstable region of a process is defined by:

$$\mathcal{K} > 0 \tag{4.2}$$

As discussed in Section 3, the divergence can be positive for stable batch processes. Hence the stability criterion $\mathcal{K}$ is connected to the divergence by the following equation:

$$\mathcal{K} = \text{div}[\mathbf{J}] - |\mathcal{E}| \tag{4.3}$$

The estimate function $\mathcal{E}$ approximates the divergence value for the batch process on the boundary of instability. Since the divergence increases much more rapidly, once the system is unstable, the value of div[**J**] will increase further than $\mathcal{E}$ and hence a positive value for $\mathcal{K}$ is obtained. The stability of the system is evaluated at iteration '*i*', which is given by:

$$\mathcal{K}^{(i)} = \text{div}[\mathbf{J}]^{(i)} - |\mathcal{E}^{(i)}| \tag{4.4}$$

where

$$\mathcal{E}^{(i)} = f\left(\text{div}[\mathbf{J}]^{(i-1)}\right) \tag{4.5}$$

In order to determine if an unstable process is present, the system is simulated for 1000 s under full cooling capacity for varying parameters. The process is identified as unstable if the curvature of the temperature profile at the final time is positive, or the temperature is greater than 10 K from the initial temperature.

To derive an equation for the stability criterion $\mathcal{K}$, the divergence of the Jacobian for the system in Eqs. (2.2)–(2.7) is first given in terms of non-dimensional variables:

$$\mathrm{div}[\mathbf{J}] = \frac{1}{t_{ref}}(Da\exp(-\gamma)(B\gamma - n) - St) \tag{4.6}$$

where

$$B = \frac{(-\Delta H_r)[\mathrm{A}]}{\rho C_p T_R} \tag{4.7}$$

$$Da = k_0[\mathrm{A}]^{n-1}\,t \tag{4.8}$$

$$\gamma = \frac{E_a}{RT_R} \tag{4.9}$$

$$St = \frac{UA}{\rho C_p V}\,t \tag{4.10}$$

where B is a dimensionless adiabatic temperature rise, Da is the Damköhler number, γ is the Arrhenius number and St is the Stanton number.

The reference time t_{ref} is introduced in order to satisfy the units of divergence, which are $[\mathrm{div}[\mathbf{J}]] = [\mathrm{s}^{-1}]$, and plays no important role in further analysis. For convenience the value of t_{ref} is set to 1 s. In general the divergence is defined by:

$$\mathrm{div}[\mathbf{J}] = f\left(B, \frac{Da}{t_{ref}}, \gamma, \frac{St}{t_{ref}}\right) \tag{4.11}$$

The function for the estimate of the divergence, $\mathcal{E}$, therefore is a function of the variables $\frac{Da}{t_{ref}}, B, \gamma,$ and $\frac{St}{t_{ref}}$.

In the following analysis the effect of varying the reaction rate constant k_0, the enthalpy of reaction ΔH_r, the heat transfer coefficient U, initial reaction temperature $T_{R,0}$, the reaction order n, the activation energy E_a and initial concentration of reagent A, $[\mathrm{A}]_0$, are considered. In order to obtain a function for $\mathcal{E}$, a first order Taylor expansion of the logarithm of the divergence, $\ln(\mathrm{div}[\mathbf{J}])$, is carried out:

$$\begin{aligned}\mathrm{d}\ln(\mathrm{div}[\mathbf{J}]) = {} & \left(\frac{\partial \ln(\mathrm{div}[\mathbf{J}])}{\partial \ln(B)}\right)_{\frac{Da}{t_{ref}},\gamma,\frac{St}{t_{ref}}} \mathrm{d}\ln(B) + \left(\frac{\partial \ln(\mathrm{div}[\mathbf{J}])}{\partial \ln\left(\frac{Da}{t_{ref}}\right)}\right)_{B,\gamma,\frac{St}{t_{ref}}} \mathrm{d}\ln\left(\frac{Da}{t_{ref}}\right) \\ & + \left(\frac{\partial \ln(\mathrm{div}[\mathbf{J}])}{\partial \ln(\gamma)}\right)_{B,\frac{Da}{t_{ref}},\frac{St}{t_{ref}}} \mathrm{d}\ln(\gamma) + \left(\frac{\partial \ln(\mathrm{div}[\mathbf{J}])}{\partial \ln\left(\frac{St}{t_{ref}}\right)}\right)_{B,\frac{Da}{t_{ref}},\gamma} \mathrm{d}\ln\left(\frac{St}{t_{ref}}\right)\end{aligned} \tag{4.12}$$

The partial derivatives describe the influence of variables $\frac{Da}{t_{ref}}, B, \gamma,$ and $\frac{St}{t_{ref}}$ on the gradient of $\mathrm{div}[\mathbf{J}]$. The function $\mathcal{E}$ is supposed to correct the divergence value for stable processes, during which the divergence is positive. As the process approaches instability, function $\mathcal{E}$ should be equal to $\mathrm{div}[\mathbf{J}]$, therefore predicting the thermal runaway correctly.

The partial derivative terms from Eq. (4.12) are calculated whilst keeping the other respective variable values constant. The terms are denoted by:

$$\left(\frac{\partial \ln(\mathrm{div}[\mathbf{J}])}{\partial \ln(B)}\right)_{\frac{Da}{t_{ref}},\gamma,\frac{St}{t_{ref}}} = m_B \tag{4.13}$$

$$\left(\frac{\partial \ln(\mathrm{div}[\mathbf{J}])}{\partial \ln\left(\frac{Da}{t_{ref}}\right)}\right)_{B,\gamma,\frac{St}{t_{ref}}} = m_{Da} \tag{4.14}$$

$$\left(\frac{\partial \ln(\mathrm{div}[\mathbf{J}])}{\partial \ln(\gamma)}\right)_{B,\frac{Da}{t_{ref}},\frac{St}{t_{ref}}} = m_\gamma \tag{4.15}$$

$$\left(\frac{\partial \ln(\mathrm{div}[\mathbf{J}])}{\partial \ln\left(\frac{St}{t_{ref}}\right)}\right)_{B,\frac{Da}{t_{ref}},\gamma} = m_{St} \tag{4.16}$$

With these new coefficients, Eq. (4.12) becomes:

$$\begin{aligned}\mathrm{d}\ln(\mathrm{div}[\mathbf{J}]) = {} & m_B\,\mathrm{d}\ln(B) + m_{Da}\,\mathrm{d}\ln\left(\frac{Da}{t_{ref}}\right) + m_\gamma\,\mathrm{d}\ln(\gamma) \\ & + m_{St}\,\mathrm{d}\ln\left(\frac{St}{t_{ref}}\right)\end{aligned} \tag{4.17}$$

The differential of a logarithm is given by:

$$\mathrm{d}\ln(y) = \frac{\mathrm{d}y}{y} = \lim_{\Delta y^i \to 0}\frac{\Delta y^{(i)}}{y^{(i-1)}} \approx \frac{y^{(i)} - y^{(i-1)}}{y^{(i-1)}} \tag{4.18}$$

where the superscript i means evaluated at time step 'i'. Therefore, Eq. (4.17) can now be written as:

$$\begin{aligned}\mathrm{d}\ln(\mathrm{div}[\mathbf{J}]) = {} & \frac{\mathrm{div}[\mathbf{J}]^{(i)} - \mathrm{div}[\mathbf{J}]^{(i-1)}}{\mathrm{div}[\mathbf{J}]^{(i-1)}} \\ = {} & m_B\frac{B^{(i)} - B^{(i-1)}}{B^{(i-1)}} + m_{Da}\frac{Da^{(i)} - Da^{(i-1)}}{Da^{(i-1)}} \\ & + m_\gamma\frac{\gamma^{(i)} - \gamma^{(i-1)}}{\gamma^{(i-1)}} + m_{St}\frac{St^{(i)} - St^{(i-1)}}{St^{(i-1)}}\end{aligned} \tag{4.19}$$

Since the equation for $\mathcal{E}^{(i)}$ is the estimate of the divergence at the boundary of stability, the difference equation of the divergence criterion is used to obtain this estimate. Hence Eq. (4.19) is rearranged to obtain $\mathrm{div}[\mathbf{J}]^{(i)}$ on the left-hand-side, which becomes the expression for $\mathcal{E}^{(i)}$. This rearrangement leads to the following equation:

$$\begin{aligned}\mathcal{E}^{(i)} = {} & \mathrm{div}[\mathbf{J}]^{(i-1)}\left(1 + m_B\frac{B^{(i)} - B^{(i-1)}}{B^{(i-1)}} + m_{Da}\frac{Da^{(i)} - Da^{(i-1)}}{Da^{(i-1)}}\right. \\ & \left. + m_\gamma\frac{\gamma^{(i)} - \gamma^{(i-1)}}{\gamma^{(i-1)}} + m_{St}\frac{St^{(i)} - St^{(i-1)}}{St^{(i-1)}}\right)\end{aligned} \tag{4.20}$$

The stability criterion $\mathcal{K}$ can now be evaluated as the difference of the actual divergence of the Jacobian and the correction function at time step i:

$$\mathcal{K}^{(i)} = \mathrm{div}[\mathbf{J}]^{(i)} - \left|\mathcal{E}^{(i)}\right| \tag{4.21}$$

Eq. (4.21) in completely written out format is given as:

$$\begin{aligned}\mathcal{K}^{(i)} = {} & \mathrm{div}[\mathbf{J}]^{(i)} - \left|\mathrm{div}[\mathbf{J}]^{(i-1)}\left(1 + m_B\frac{B^{(i)} - B^{(i-1)}}{B^{(i-1)}} + m_{Da}\frac{Da^{(i)} - Da^{(i-1)}}{Da^{(i-1)}}\right.\right. \\ & \left.\left. + m_\gamma\frac{\gamma^{(i)} - \gamma^{(i-1)}}{\gamma^{(i-1)}} + m_{St}\frac{St^{(i)} - St^{(i-1)}}{St^{(i-1)}}\right)\right|\end{aligned} \tag{4.22}$$

The values of coefficients $m_B, m_{Da}, m_\gamma,$ and m_{St} are evaluated in the next section.

4.2. Derivation of coefficients

The coefficients m_B, m_{Da}, m_γ and m_{St} are evaluated as the gradients of the function $\ln(\mathrm{div}[\mathbf{J}])$ with respect to variables B, Da, γ and St where the system becomes unstable for processes P_1—P_{15}.

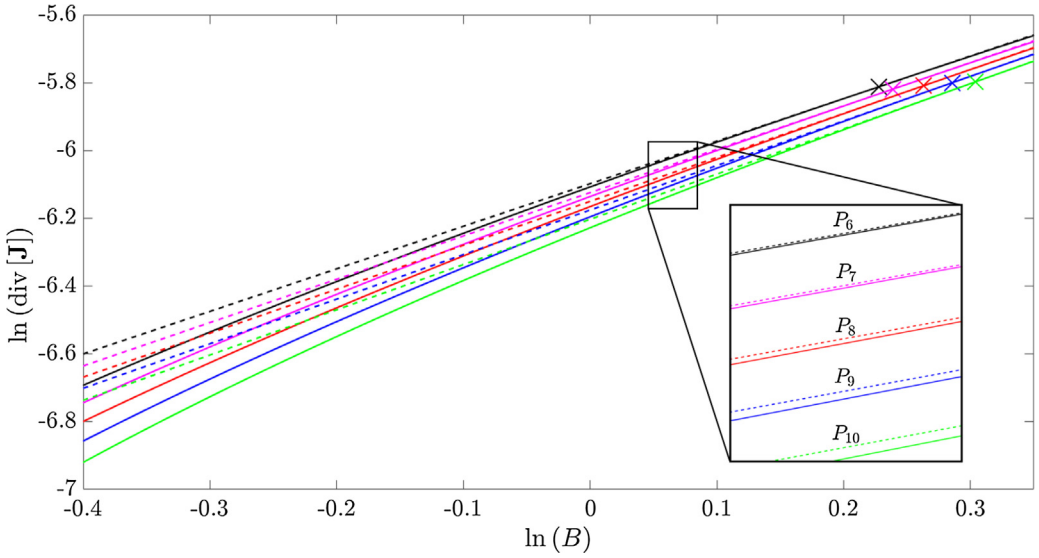

Fig. 6. Variation of the divergence with respect to B for processes P_6—P_{10}. The crosses indicate the points at the boundary of instability, and the dashed lines indicate the gradient at these points.

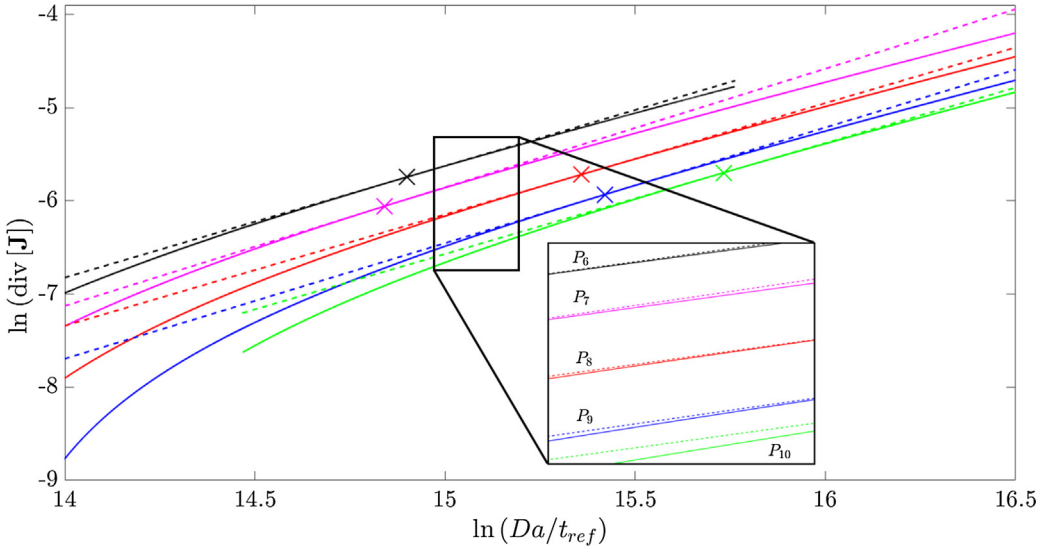

Fig. 7. Variation of the divergence with respect to Da/t_{ref} for processes P_6—P_{10}. The crosses indicate the points at the boundary of instability, and the dashed lines indicate the gradient at these points.

The first coefficient m_B is evaluated at the boundary of stability while keeping the values of $\frac{Da}{t_{ref}}$, γ and $\frac{St}{t_{ref}}$ constant, as shown in Eq. (4.13). The gradients of $\ln(\mathrm{div}[\mathbf{J}])$ with respect to $\ln(B)$ for processes P_6—P_{10} are shown in Fig. 6.

From Fig. 6 it can be seen that the gradients at the boundary of instability are approximately parallel for processes P_6—P_{10}. A similar result is obtained for processes P_1—P_5 and P_{11}—P_{15} for the variation of $\ln(\mathrm{div}[\mathbf{J}])$ with $\ln(B)$.

The second coefficient m_{Da} is evaluated at the boundary of stability while keeping the values of B, γ and St/t_{ref} constant, as shown in Eq. (4.14). The gradients of $\ln(\mathrm{div}[\mathbf{J}])$ with respect to $\ln\left(\frac{Da}{t_{ref}}\right)$ for processes P_6—P_{10} are shown in Fig. 7.

In Fig. 7 it can be seen that the values of Da/t_{ref}, at which the system becomes unstable, is different for each process. The gradients obtained at these points are still approximately parallel for processes P_6—P_{10}. Similar results are obtained for processes P_1—P_5 and P_{11}—P_{15}.

The third coefficient m_γ is evaluated at the boundary of stability while keeping the values of B, Da/t_{ref} and St/t_{ref} constant, as shown in Eq. (4.15). The gradients of $\ln(\mathrm{div}[\mathbf{J}])$ with respect to $\ln(\gamma)$ for processes P_6—P_{10} are shown in Fig. 8.

The values of γ at which processes P_6—P_{10} becomes unstable are different for each process. Still, the gradients of $\ln(\mathrm{div}[\mathbf{J}])$ at these points are parallel as can be seen in Fig. 8. The same conclusions can be made about the results obtained for processes P_1—P_5 and P_{11}—P_{15}.

The fourth coefficient m_{St} is evaluated at the boundary of stability while keeping the values of B, γ and Da/t_{ref} constant, as shown in Eq. (4.16). The gradients of $\ln(\mathrm{div}[\mathbf{J}])$ with respect to $\ln\left(\frac{St}{t_{ref}}\right)$ for processes P_6—P_{10} are shown in Fig. 9.

The gradients obtained at the point of instability for the variable St/t_{ref} are again approximately parallel for processes P_6—P_{10}. As was the case for the calculations of the previous three coefficients there is a good match for m_{St} obtained for processes P_1—P_5 and P_{11}—P_{15}.

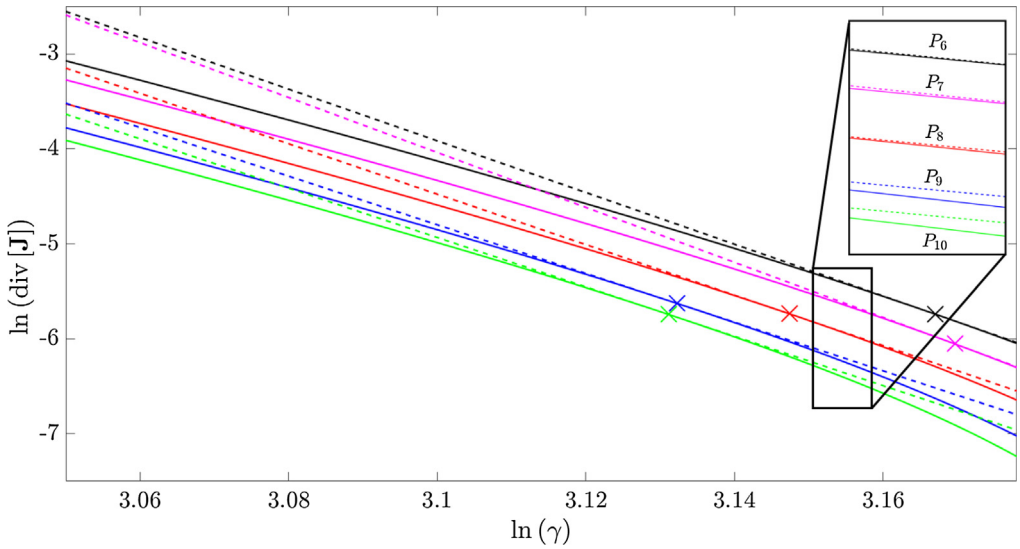

Fig. 8. Variation of the divergence with respect to γ for processes P_6—P_{10}. The crosses indicate the points at the boundary of instability, and the dashed lines indicate the gradient at these points.

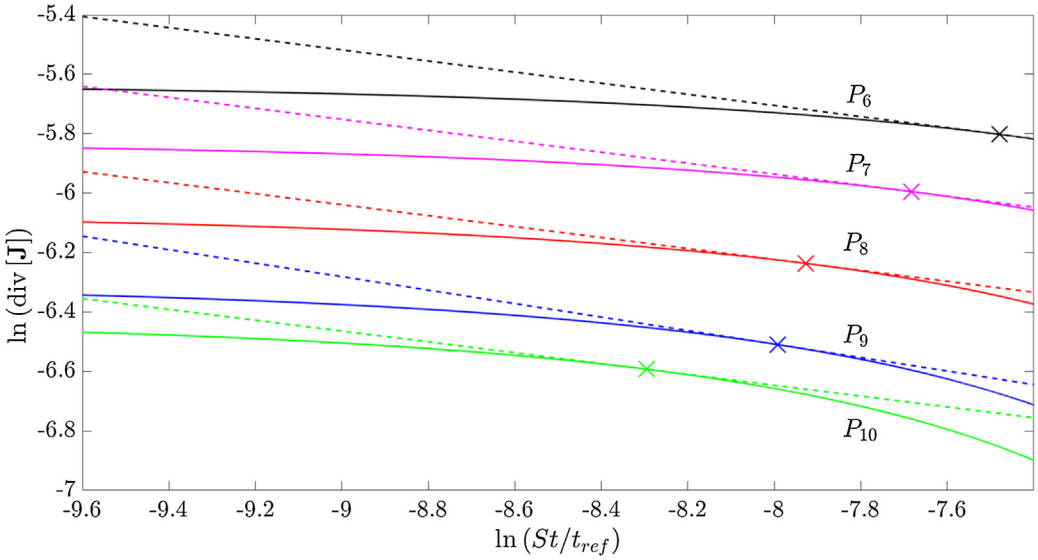

Fig. 9. Variation of the divergence with respect to St/t_{ref} for processes P_6—P_{10}. The crosses indicate the points at the boundary of instability, and the dashed lines indicate the gradient at these points.

If the gradients are parallel, the gradient coefficients obtained are very close to each other, hence making the assumption of using a single value of m reasonable in order to characterise the behaviour of the batch reactor system at the boundary of stability. The fact that the lines obtained for each variable give a very similar gradient value is promising and gives a good foundation for the use of the stability criterion $\mathcal{K}$.

The coefficient values with their averages and deviations are summarised in Table 7.

One source of the deviations for coefficients m_B, m_{Da}, m_γ and m_{St} is the determination of when a process becomes unstable, as there is no clear definition of when a thermal runaway occurs.

Due to the variation of variables B, Da, γ and St in a broad spectrum the coefficients m_B, m_{Da}, m_γ and m_{St} are valid for the stability function of exothermic batch processes with reaction kinetics mainly dependent on a single component.

Now the values of the coefficients in Eq. (4.22) can be introduced:

$$\mathcal{K}^{(i)} = \mathrm{div}[\mathbf{J}]^{(i)} - \left|\mathrm{div}[\mathbf{J}]^{(i-1)}\left(1 + 1.28\frac{B^{(i)} - B^{(i-1)}}{B^{(i-1)}} + 1.21\frac{Da^{(i)} - Da^{(i-1)}}{Da^{i-1}} - 26.9\frac{\gamma^{(i)} - \gamma^{(i-1)}}{\gamma^{(i-1)}} - 0.187\frac{St^{(i)} - St^{(i-1)}}{St^{(i-1)}}\right)\right| \tag{4.23}$$

The profiles of $\mathcal{K}$ for all processes P_1—P_5 are plotted in Fig. 10.

It can be seen in Fig. 10 that the new stability criterion $\mathcal{K}$ gives a much better prediction of the system stability than the divergence on its own, as can be seen in Fig. 4. The values of $\mathcal{K}$ at the boundary of stability for processes P_1—P_{15} are given in Table 8.

The values for $\mathcal{K}$ obtained for processes P_1–P_{15}, as reported in Table 8, are at the point of where each process is unstable. Therefore a positive value of $\mathcal{K}$ indicates an unstable process is present.

Table 7
Values of coefficients for processes P_1—P_{15}. Averages and deviations are also given.

Process	m_B	m_γ	m_{Da}	m_{St}	Process	m_B	m_γ	m_{Da}	m_{St}
P_1	1.24	−27.0	1.19	−0.187	P_{10}	1.33	−26.0	1.19	−0.180
P_2	1.27	−26.9	1.19	−0.186	P_{11}	1.26	−27.3	1.20	−0.189
P_3	1.29	−26.9	1.19	−0.186	P_{12}	1.26	−27.2	1.20	−0.191
P_4	1.24	−26.8	1.19	−0.187	P_{13}	1.26	−27.2	1.20	−0.187
P_5	1.33	−27.0	1.19	−0.184	P_{14}	1.26	−27.2	1.20	−0.188
P_6	1.25	−27.2	1.21	−0.191	P_{15}	1.26	−27.2	1.20	−0.188
P_7	1.38	−27.0	1.27	−0.185					
P_8	1.30	−26.6	1.20	−0.184	Average	1.28	−26.9	1.21	−0.187
P_9	1.32	−26.0	1.19	−0.182	Deviation	±0.07	±0.67	±0.04	±0.01

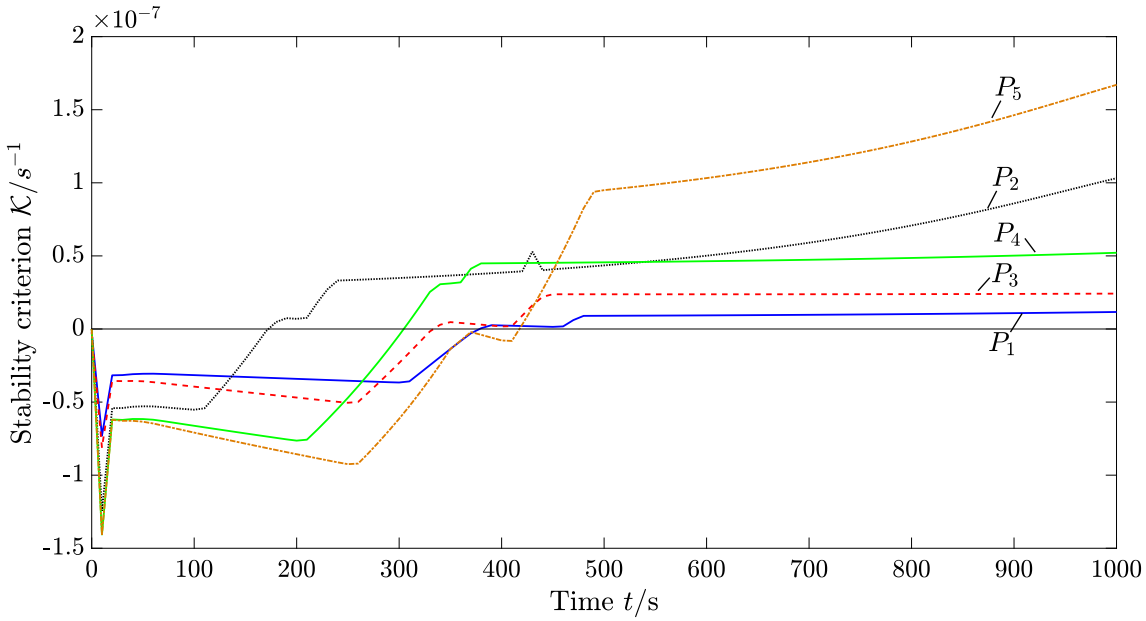

Fig. 10. Stability criterion $\mathcal{K}$ profiles for Processes P_1—P_5.

Table 8
Values of $\mathcal{K}$ at the boundary of stability for processes P_1—P_{15}.

Process	$\mathcal{K}/10^{-8}$ [s^{-1}]	Process	$\mathcal{K}/10^{-8}$ [s^{-1}]	Process	$\mathcal{K}/10^{-8}$ [s^{-1}]
P_1	0.90	P_6	1.03	P_{11}	4.51
P_2	2.28	P_7	3.07	P_{12}	4.24
P_3	2.20	P_8	2.10	P_{13}	1.98
P_4	4.49	P_9	1.07	P_{14}	1.52
P_5	6.56	P_{10}	1.70	P_{15}	1.49

Ideally, at the point of instability, criterion $\mathcal{K}$ should give a value of zero. Since criterion $\mathcal{K}$ depends on the linear estimate of the divergence at the boundary of stability, given by $\mathcal{E}$, the reliability of $\mathcal{K}$ depends on how accurately the boundary of stability can be determined.

The stability criterion $\mathcal{K}$ enables a clear description of the change from a stable to an unstable condition of batch reactions, since a sign change occurs when the process becomes unstable (see Fig. 10). The difference between div[**J**] and $\mathcal{K}$ at the point of instability does not seem to be significant at first sight $\left(10^{-3}\text{ in comparison to }10^{-8}\right)$, but the value of criterion $\mathcal{K}$ becomes positive when the system turns unstable, which is not the case for the divergence criterion. When applied as a stability criterion for MPC, as is shown in the next section, the implementation of div[**J**] and $\mathcal{K}$ leads to drastic differences in efficiency for batch reactions.

The application of criterion $\mathcal{K}$ therefore plays a key role in embedding an online stability measure with MPC for batch reactions. The implementation of function $\mathcal{K}$ and the divergence criterion with MPC are shown in the following section.

5. MPC with integrated stability analysis

The analysis of stability of batch processes is incorporated into the classical MPC flow sheet, which is shown in Fig. 11.

Model Predictive Control (MPC) is an advanced control scheme, in which an Optimal Control Problem is solved iteratively (Chuong La et al., 2017; Mayne, 2014). The mathematical formulation for MPC used in this work is given by (Charitopoulos and Dua, 2016; Rawlings and Mayne, 2015):

$$\min_{q_C(\cdot)} \Phi(x(t), q_C(t)) \tag{5.1}$$

subject to the system described in Eqs. (2.2)–(2.7) and:

$$\Phi = \int_{t_0}^{t_f} \left(T_R(t) - T_{sp}(t)\right)^2 dt \tag{5.2}$$

$$h(x(t), q_C(t), t) = 0 \tag{5.3}$$

$$\mathcal{K} \leqslant 0 \tag{5.4}$$

$$T_R \leqslant T_{chem} \tag{5.5}$$

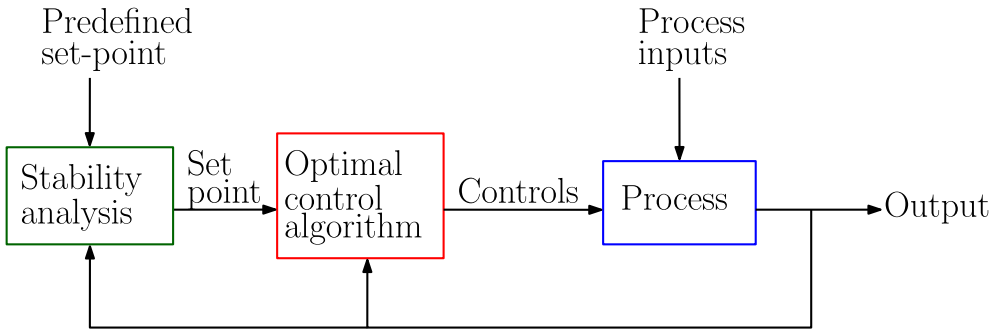

Fig. 11. Model Predictive Control scheme with integrated stability analysis.

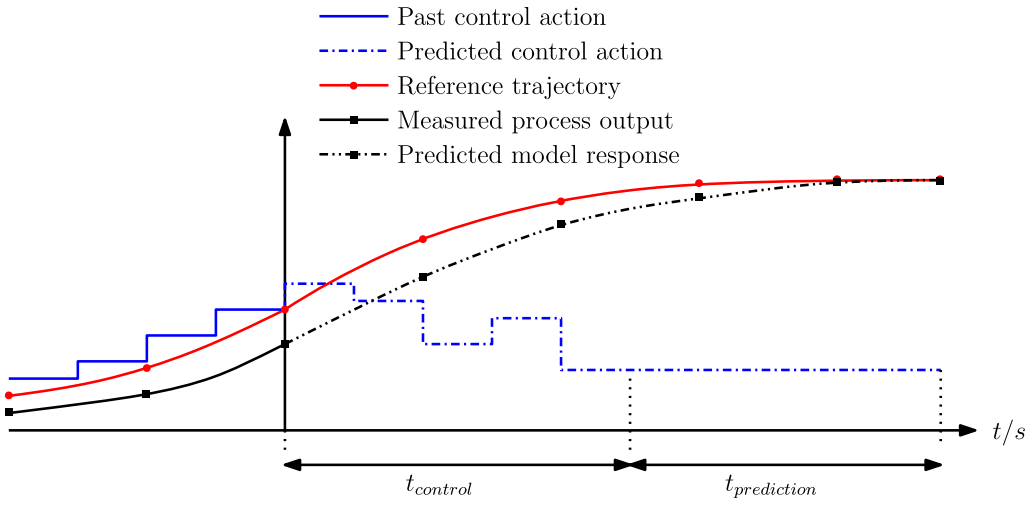

Fig. 12. Diagram of Model Predictive Control horizons $t_{control}$ and $t_{prediction}$, which influence the performance of the algorithm.

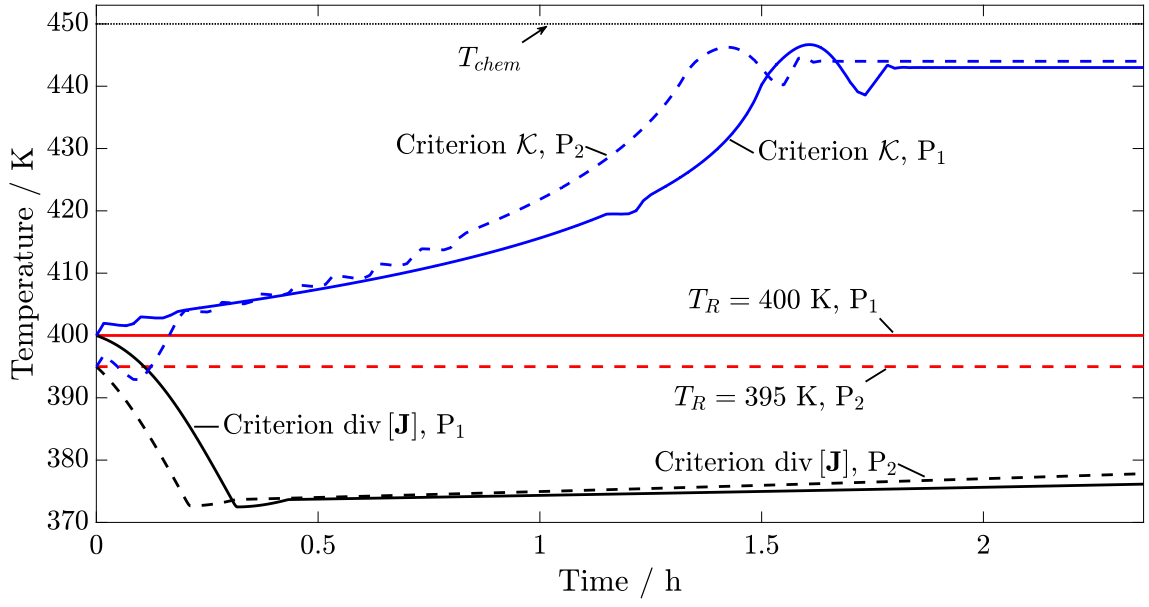

Fig. 13. Temperature profiles for batch processes P_1 and P_2 with MPC and integrated stability measures.

$$0 \leqslant q_C \leqslant q_{C,max} \tag{5.6}$$

$$t_0 \leqslant t \leqslant t_f \tag{5.7}$$

where $h(x(t), q_C(t), t)$ are the equations giving the physical properties, the initial time and final time of the simulation are set to $t_0 = 0$ s and $t_f = 8500$ s, respectively, and the chemical stability

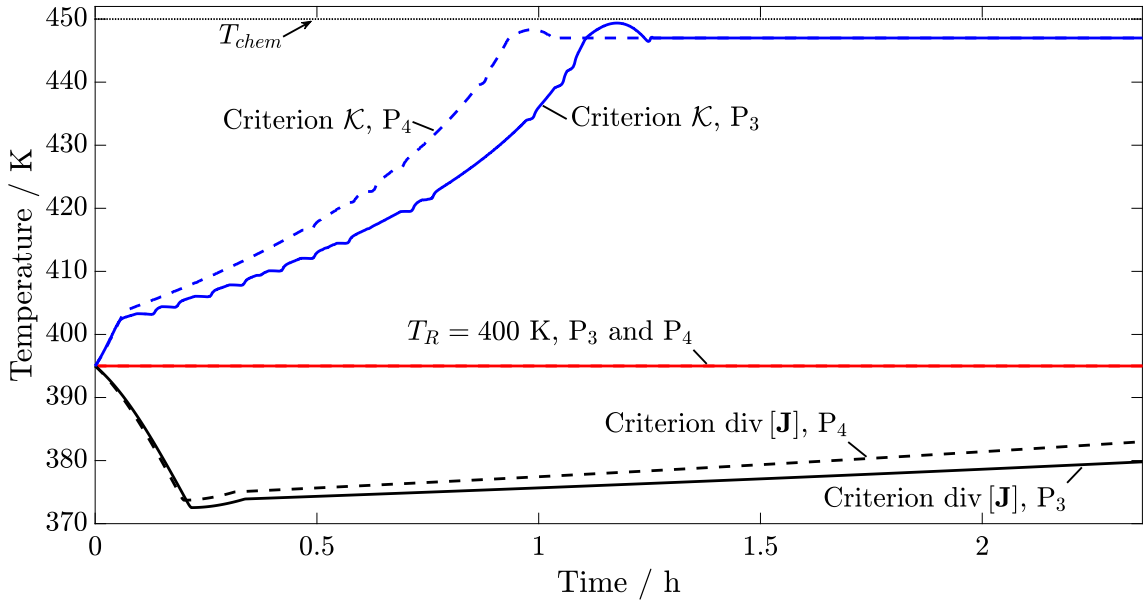

Fig. 14. Temperature profiles for batch processes P_3 and P_4 with MPC and integrated stability measures.

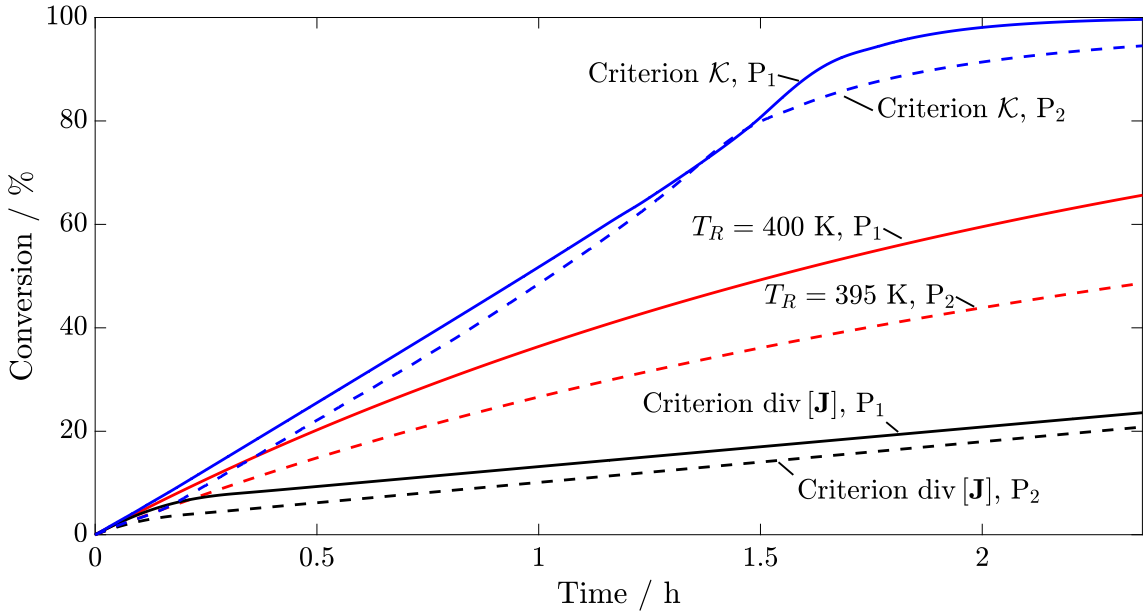

Fig. 15. Conversion profiles for batch processes P_1 and P_2 with MPC and integrated stability measures.

temperature is set to $T_{chem} = 450$ K. The constraint $\mathcal{K} \leqslant 0$ in Eq. (5.4) ensures that the process does not enter an unstable region.

The problem given in Eqs. (5.1)–(5.7) is solved using the SQP optimisation (Nocedal and Wright, 2006) algorithm within *fmincon* in MATLAB™. The implementation of the optimal control problem solution with the nonlinear MPC framework was sequential. The selection of the final time of simulation t_f gives rise to a trade-off: The final time of the MPC scheme has to be chosen long enough to capture the thermal runaway, but short enough to not increase detrimentally the computational cost.

The algorithm proceeds with a "moving horizon": At time t the optimal control action is evaluated for a control and prediction horizon of $t_{control}$ and $t_{prediction}$, respectively. This scheme is shown diagrammatically in Fig. 12.

The control action found by the optimisation algorithm is implemented only for the first step. After every iteration the algorithm is fed with new process data, which together with the included process model lead to new predictions of the system behaviour. According to the data and the process model, the optimisation is carried out to find the optimal control values.

In literature most Model Predictive Control schemes implement a linearisation of the system present, with which a linear MPC scheme can be used (Rawlings and Mayne, 2015). With such a formulation the stability of the closed-loop system can be proven theoretically by the use of Lyapunov functions (DeHaan and Guay, 2010; Huang et al., 2012). If no Lyapunov function can be found, end-point constraints are often employed for a very large prediction horizon. For complex and highly nonlinear systems this leads to higher computational cost as the system has to be simulated for a larger time frame. The use of an online stability criterion can reduce the time frame used by giving an indication of the system stability at each point of the simulation.

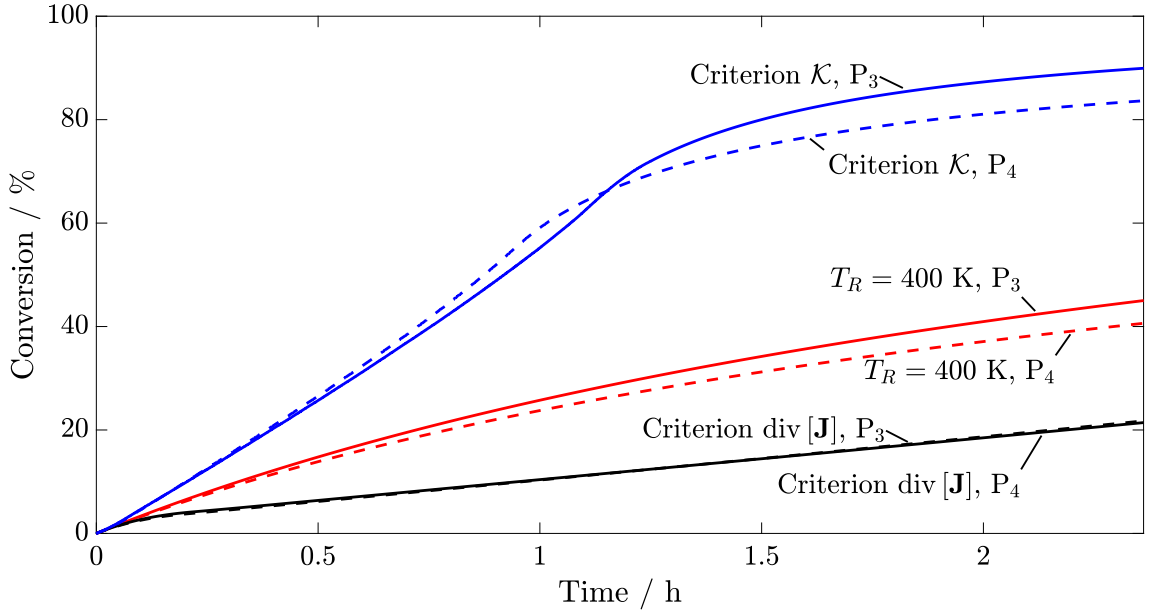

Fig. 16. Conversion profiles for batch processes P_3 and P_4 with MPC and integrated stability measures.

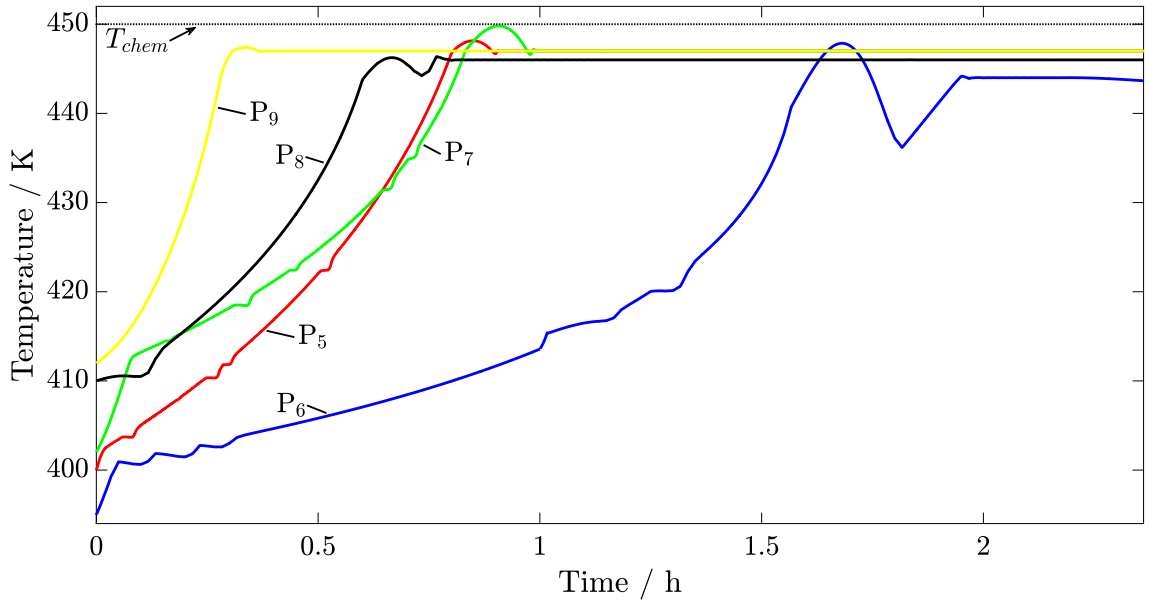

Fig. 17. Temperature profiles for processes P_5—P_9 with MPC using stability criterion $\mathcal{K}$.

In the simulations shown below a control horizon of $t_{control} = 100$ s with 5 equally long control steps, and a prediction horizon of $t_{prediction} = 20$ s are used. During each control step the value of the control variable is unchanged, which is equivalent to a zero order hold element (Haber et al., 2011).

An increase in the efficiency of batch processes can be achieved with MPC, as long as the process stays stable. In the following case studies all processes, the parameters of which are given in Tables 4 and 5, are applied to Model Predictive Control. For the processes simulated the effectiveness of using stability criterion $\mathcal{K}$ over using the divergence criterion or keeping a constant temperature set-point during the process is shown.

The temperature profiles of processes P_1—P_4 for MPC using the stability criterion $\mathcal{K}$, the divergence criterion div[**J**] and keeping a constant temperature are shown in Figs. 13 and 14.

The initial temperature of the processes in Figs. 13 and 14 is close to the boundary of instability. It can be seen that batch processes with MPC and integrated stability criterion $\mathcal{K}$ can lead to an increase in temperature during the process. If instead criterion div[**J**] is used the temperature is first decreased unnecessarily, because the criterion detects an unstable process. If the temperature in the process is kept constant, which can be done by a PI controller, the reaction will be slower. Hence a more efficient process is obtained when implementing criterion $\mathcal{K}$.

The conversion of reagent A for MPC using the stability criterion $\mathcal{K}$, the divergence criterion div[**J**] and keeping a constant temperature is shown in Figs. 15 and 16.

The conversion increases much faster for processes with MPC including stability criterion $\mathcal{K}$ than for the processes with MPC and the divergence criterion or for processes with a constant

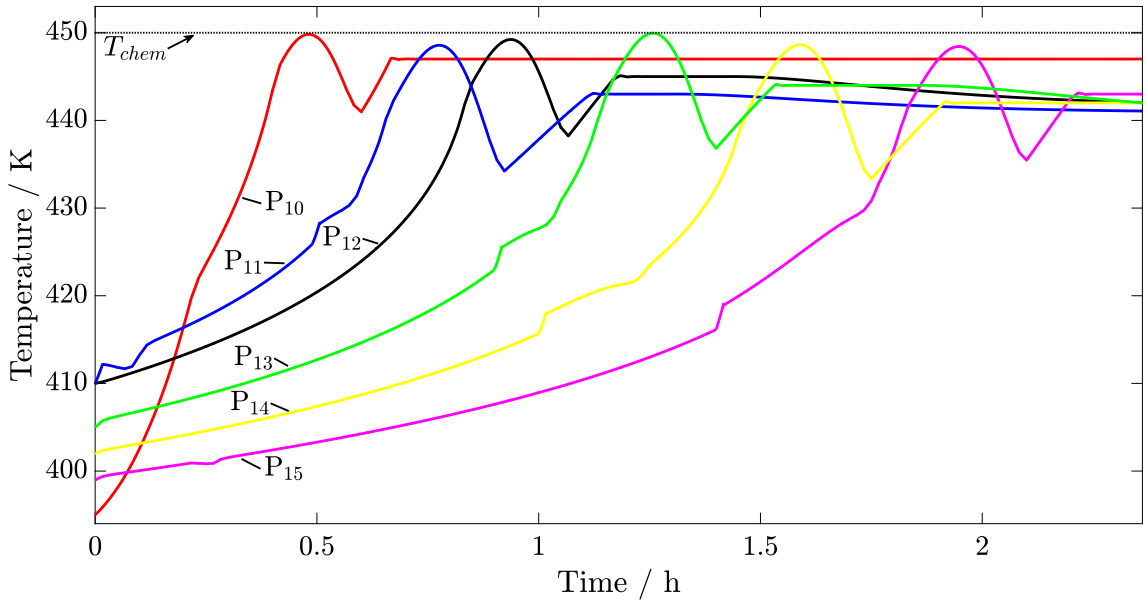

Fig. 18. Temperature profiles for processes P_{10}—P_{15} with MPC using stability criterion $\mathcal{K}$.

reaction temperature. In the case of using the criterion $\mathcal{K}$ a set point temperature just below T_{chem} can be used. The MPC algorithm keeps the system in the stable region by continuously satisfying the constraint in Eq. (5.4), therefore avoiding thermal runaway reactions.

From Figs. 13–16 it can be seen clearly that implementing the divergence criterion in an MPC scheme results in an overly conservative process. To show that the implementation of stability criterion $\mathcal{K}$ results in a controlled, intensified batch process, an MPC scheme using criterion $\mathcal{K}$ for all remaining processes is implemented. The corresponding temperature profiles for processes P_5—P_{15} are shown in Figs. 17 and 18.

It can be seen from Figs. 17 and 18 that for each process the system can be intensified, while keeping the process under control. The additional constraint of a maximum chemical temperature to avoid possible side reactions can be incorporated also into the advanced control scheme, as is shown in the above case studies.

For an efficient application of MPC with an integrated stability criterion $\mathcal{K}$ into process control the time required for the calculations is crucial. On average the evaluation of the control action for the next iteration step required approximately 20 s, which is currently too slow for implementation. With the use of more efficient solvers and tuning of the control and prediction horizons, a faster implementation for MPC can be achieved.

6. Conclusions

A batch reaction model was introduced with PI control, for which several simulations were carried out. The systems, initially stable, were made unstable by increasing the temperature set point. The performance of the divergence criterion commonly found in literature (Strozzi and Zaldívar, 1994) was tested and it was found that this criterion gives no clear indication of when a system turns unstable.

The new stability criterion $\mathcal{K}$ was introduced, which is based on the definition of the divergence criterion. The derivation is based on a linear approximation of the divergence for the batch reaction system. The stability coefficients obtained from the linearisation are evaluated and applied to the same simulations. It was found that a clear indication of when the system turns unstable is present.

Model Predictive Control (MPC) was introduced and the stability criterion $\mathcal{K}$ was integrated into the MPC scheme. This control algorithm was compared to an MPC scheme including the divergence criterion. It was found that the resulting control profiles including the criterion $\mathcal{K}$ showed much better performance than the systems including the divergence criterion. It was further shown that if the divergence criterion is used the process becomes very inefficient, as the divergence criterion gives a very conservative estimate of the system stability. If no temperature increase is present during the batch reaction, the process is stable, but not as efficient as with the embedding of criterion $\mathcal{K}$. Hence the implementation of criterion $\mathcal{K}$ improves the batch reaction system.

This work has presented a totally new way of stabilising thermal runaway systems with an online MPC algorithm. The benefits demonstrated by the case studies presented demonstrate the benefits over traditional control approaches, as well as the enhanced ability to intensify the underlying processes so as to achieve greater productivity.

The contribution of this work is to pave the way for more suitably tailored criteria incorporating stability into online control algorithms that enhance safety and performance of processes that can become unstable with detrimental effects and lead to economic loss. Future work will focus on implementing stability criterion $\mathcal{K}$ to more complex reaction kinetics of batch and semi-batch reactors. More advanced Model Predictive Control schemes will be implemented to speed up the time required for each iteration.

The new stability criterion uses second order derivatives, as opposed to the original divergence criterion which uses first order derivatives, hence making criterion $\mathcal{K}$ computationally more expensive. Nonetheless it is important not to miss the point put forward in this work: the original divergence criterion in and of itself is often proven to be either too conservative or unreliable for batch processes. As such, the extra cost and effort for the computations required make criterion $\mathcal{K}$ seem to be worth the effort.

The computational cost, as well as accuracy, of using numerical differentiation with the divergence criterion and stability criterion $\mathcal{K}$ will hence be analysed in future work.

The effect of uncertainty in process parameters and model-plant-mismatch on the reliability of stability criterion $\mathcal{K}$ have to be considered for future case studies. The robustness of stability

criteria for online applications is of major importance and hence needs consideration in future work.

This will enable the stability criterion $\mathcal{K}$ to be used in control schemes for industry.

Acknowledgments

We thank the Engineering and Physical Sciences Research Council (EPSRC) and the Department of Chemical Engineering and Biotechnology, University of Cambridge, for funding this project.

References

Arnold, V., 1973. Ordinary Differential Equations. MIT Press, Cambridge, MA, pp. 95–208 (Chapter 3).
Barkelew, C., 1959. Stability of chemical reactors. Chem. Eng. Prog. Symp. Ser. 25, 37–46.
Bohne, D., Fischer, S., Obermeier, E., 2010. Thermal conductivity, density, viscosity, and Prandtl-numbers of ethylene glycol-water mixtures. Berich. Bundesgesellschaft Phys. Chem. 88 (8), 739–742.
Bosch, J., Strozzi, F., Zbilut, J., Zaldívar, J.M., 2004. On-line runaway detection in isoperibolic batch and semibatch reactors using the divergence criterion. Comput. Chem. Eng. 28 (4), 527–544.
Charitopoulos, V.M., Dua, V., 2016. Explicit model predictive control of hybrid systems and multiparametrix mixed integer polynomial programming 62, 3441–2460.
Chuong La, H., Potschka, A., Bock, H.G., 2017. Partial stability for nonlinear model predictive control. Automatica 78, 14–19.
Copelli, S., Torretta, V., Pasturenzi, C., Derudi, M., Cattaneo, C., Rota, R., 2014. On the divergence criterion for runaway detection: application to complex controlled systems. J. Loss Prev. Process Ind. 28, 92–100.
Crittenden, J.C., Trussell, R.R., Hand, D.W., Howe, K.J., Tchobanoglous, G., 2012. MWH's Water Treatment: Principles and Design, third ed. John Wiley & Sons, pp. 1861–1862 (Chapter Appendix C).
Davis, M., Davis, R., 2003. Fundamentals of Chemical Reaction Engineering. McGraw-Hill, pp. 53–56 (Chapter 2).
DeHaan, D., Guay, M., 2010. Model Predictive Control. Sciyo, pp. 26–58 (Chapter 2).
Dever, J., George, K., Hoffman, W., Soo, H., 2004. Kirk-Othmer Encyclopedia of Chemical Technology. John Wiley & Sons, pp. 632–673 (Chapter Ethylene Oxide).
Green, D.W., Perry, R.H., 2008. Perry's Chemical Engineers' Handbook, eighth ed. The McGraw-Hill (Chapter 2).
Haber, R., Bars, R., Schmitz, U., 2011. Predictive Control in Process Engineering. Wiley-VCH Verlag GmbH & Co. KGaA, pp. 29–54 (Chapter 2).
Hirschfelder, J.O., Curtiss, C.F., Bird, R.B., 1955. Molecular theory of gases and liquids. Am. Inst. Chem. Eng. J. 1 (2), 272.
Huang, R., Biegler, L.T., Harianth, E., 2012. Robust stability of economically oriented infinite horizon nmpc that include cyclic processes. J. Process Control 22, 51–59.
Mayne, D.Q., 2014. Model predictive control: recent developments and future promise. Automatica 50, 2967–2986.
Melcher, A., 2003. Numerische berechnung der lyapunov-exponenten bei gewöhnlichen differentialgleichungen (Ph.D. Thesis). Universität Karlsruhe, Fakultät für Mathematik.
Nocedal, J., Wright, S., 2006. Numerical Optimization. Springer, pp. 526–572 (Chapter 18).
Rawlings, J., Mayne, D., 2015. Model Predictive Control: Theory and Design. Nob Hill Publishing, pp. 1–60 (Chapter 1).
Rossi, F., Copelli, S., Colombo, A., Pirola, C., Manenti, F., 2015. Online model-based optimization and control for the combined optimal operation and runaway prediction and prevention in (fed-)batch systems. Chem. Eng. Sci. 138, 760–771.
Semenov, N., 1940. Thermal theory of combustion and explosion. In: Progress of Physical Science (U.S.S.R), vol. 23.
Shampine, L., Reichelt, M., Kierzenka, J., 1999. Solving index-1 daes in matlab and simulink. SIAM Rev. 41, 538–552.
Sinnot, R., 2005. Chemical Engineering Design, vol. 6. Elsevier Butterworth-Heinemann, pp. 634–638 (Chapter 12).
Stephanopoulos, G., 1984. Chemical Process Control. PTR Prentice Hall, pp. 258–279 (Chapter 14).
Strozzi, F., Zaldívar, J., 1994. A general method for assessing the thermal stability of batch chemical reactors by sensitivity calculation based on Lyapunov exponents. Chem. Eng. Sci. 49 (16), 2681–2688.
Strozzi, F., Zaldívar, J., 1999. On-line runaway detection in batch reactors using chaos theory techniques. AIChE 45 (11), 2429–2443.
Teja, A.S., 1983. Simple method for the calculation of heat capacities of liquid mixtures. J. Chem. Eng. Data 28, 83–85.
Westerterp, K., Molga, E., 2006. Safety and runaway prevention in batch and semibatch reactors: a review. Chem. Eng. Res. Des. 84 (7), 543–552.
Winde, M., 2009. Systematische bewertung und ertüchtigung von industriellen regelkreisen in verfahrenstechnischen komplexen (Ph.D. Thesis). Ruhr-Universität Bochum, Fakultät für Maschinenbau.